



# Free vibration, Buckling and Bending investigation of bidirectional FG curved sandwich beams

Mohamed Sekkal <sup>a, b</sup>, Wafa Tebboune <sup>c</sup>, Ouahiba Taleb <sup>d</sup>, Rabbab Bachir Bouiadjra <sup>a</sup>, Samir Benyoucef <sup>a</sup>, Abdelouahed Tounsi <sup>a, e, f\*</sup>

<sup>a</sup> *Material and Hydrology Laboratory, University of Sidi Bel Abbes, Faculty of Technology, Civil Engineering Department, Algeria*

<sup>b</sup> *University Ahmed Zabana of Relizane, Algeria*

<sup>c</sup> *Department of Civil Engineering, Faculty of Architecture and Civil Engineering, University of Sciences and Technology Mohamed Boudiaf, Oran 31000, Algeria*

<sup>d</sup> *University Belkaid Abou Bekr of Tlemcen, Algeria*

<sup>e</sup> *Department of Civil and Environmental Engineering, King Fahd University of Petroleum & Minerals, 31261 Dhahran, Eastern Province, Saudi Arabia*

<sup>f</sup> *Department of Civil and Environmental Engineering, Lebanese American University, 309 Bassil Building, Byblos, Lebanon*

## Abstract

The present work is focused on the bending, buckling and free vibration analysis of BDFG (bidirectional functionally graded) sandwich beams using a quasi-3D analytical solution. The present formulation is based on a displacement field that includes indeterminate terms and involves a few variables to define. The BDFG beam consists of functionally graded (FG) skins at the bottom and top with isotopic core in the middle. The materials characteristics of the skins are continuously distributed through the thickness and the length of the beam based on a specified power law. The governing equations of the simply supported curved beam are derived using the principal of virtual works and are then solved utilizing the Navier solution. The exactness of the proposed formulation is assessed by checking their numerical results with other of reliable publications available in the literature. A detailed numerical study is presented in order to investigate the impact of several parameters such grading indexes, radius of curvature, sandwich type, BDFG beam geometry and other setting on the buckling, bending and free vibration of curved BDFG beam.

**Keywords:** Bidirectional functionally graded materials; Quasi-3D hyperbolic beam theory; Curved sandwich beam instability; Multiphysics analysis; Sustainable lightweight structures; Analytical solution; Functionally graded core-skin interface; Dynamic stability

## 1. Introduction.

Curved beams have been extensively employed in numerous engineering disciplines such as civil, mechanical, aerospace and other engineering utilizations. We can also find them in the form of golf shafts and fishing rods that take on apparently deformed shapes during use[1]. With the rapid development in material science, the functionally graded material (FGM) and in a particular the sandwich materials were adopted to the curved beams[2].

Since beams are an essential component in a structure, it is essential to perform a precise structural analysis of the behavior of curved FG beams under various applications. However, in literature, researches on curved beams are very limited. An outline of some typical works can be listed as follows.

Fereidoon et al.[3] investigated the bending response of curved sandwich beam simply supported and having FG core. The authors employed the Euler-Bernoulli beam theory (also known as classical beam theory (CBT)) for the thin face-sheets and high-order shear theory (HSDT) to model the core layer. Stoykov [4] used the CBT to study the buckling of curved beam. The system of the nonlinear algebraic equation has been solved by Newton-Raphson's method. Mohamed et al.[5] studied the nonlinear forced and free vibrations of Euler-Bernoulli curved beams lying on nonlinear elastic foundations around post buckling configuration.

Li et al.[6] employed a mixed finite element (FE) approach based on the First-Order shear theory (FSDT) for the nonlinear investigation of FG curved beams. In another work, Li et al.[7] proposed a FEM formulation for geometrically nonlinear examination of FG curved beams having discontinuous stiffness. The generalized differential quadrature method (GDQM) in conjunction with the FSDT were employed by Kurtaran [8] to predict nonlinear static and dynamic response of FG curved beams having constant curvature. The Timoshenko beam theory was used by Wan et al.[1] to investigate the geometrically nonlinear response of FG curved beams having variable curvatures. The beams were exposed to thermomechanical loading. Transverse normal stress and strain were considered in sinusoidal solution proposed by Sayyad and Ghugal [9] for the static behavior of FG sandwich curved beam under uniform load.

The trigonometric shear deformation beam theory (TSDBT) was employed by Jun et al.[10] to investigate the free vibration response of laminated composite shallow curved beams. The authors used also the dynamic stiffness method to find the modes shapes and natural frequencies of these beams.

In the framework of the NURBS based isogeometric analysis, Luu and Lee[11] studied the buckling and post buckling of elliptical curved beams. Ye et al. [12]used a 2D kinematics relations for the vibration characteristics of thick laminated and sandwich composite curved beams with varying curvatures and general stresses. The flexural behaviour of multilayered curved beams having constant curvature was investigated by Thurnherr et al. [13]employing higher order beam formulation.

Avhad and Sayyad [14] presented a quasi-3D higher order shear deformation theory (HSDT) to examine the static bending of FG sandwich curved beams under uniform load. Belarbi et al. [15] presented a FE formulation based on a HSDT with three-unknown functions for the buckling response of FG curved sandwich beams. Using the same methodology, and in another work, Belarbi et al. [16]studied the static bending of FG curved sandwich beams. Eroglu [17] examined the large in-plane deflection of curved planar FG beams. Lezgy-Nazargah [18] investigated the bending of curved thin-walled beams by proposing a FE model with thirteen DOFs. Using the nonlocal elasticity theory, buckling, free vibration and bending behaviour of curved nano beams have been examined by authors of Refs [19-21]. In Ref [22], authors carried out elasticity solution based on Airy stress function method for multilayered orthotropic FG curved beams subjected to a uniform load. Sahoo et al. [23] presented a FE solution based on 2D- HSDT-kinematics field for the thermal post-buckling FG sandwich curved structure subjected to variable thermal loads.

All the above-described models have been employed to investigate the mechanics of curved FG structures with radially/thickness graded characteristics. However, for some structures working under extremely severe conditions such as aerospace craft and shuttles, the distribution of stress and temperature in the FG structures are not in one direction but in two or three. As a result, these structures are not suitable.

Consequently, scientists developed new FG structures with characteristics changing in two or three directions. The bi-direction functionally graded materials (BDFG), with characteristics changing in two directions, have better properties than those composed of a directional FGM due to the mechanical behavior which can be adapted both in the axial and thickness directions. Lately, BDFG structures have received a lot of attention [24-26].

Pydah and Sabale [27] employed the CBT for the static bending of BDFG circular beams. In another study, Pydah and Batra [28] extended the previous work by using a logarithmic function of the radial coordinate in the postulated expression of the circumferential displacement. Using the same methodology, Fariborz and Batra [29] studied the free vibration of BDFG circular beams of different opening angles and having several boundary conditions. However, one can be noted that studies on BDFG curved beams are very rare.

To the best author's experience, study on the buckling, bending and free vibration of BDFG curved sandwich beams based on a quasi-3D formulation have not been yet reported. This study presents, for the first time, an investigation on the behavior of BDFG curved simply supported sandwich beams.

The aim of this work is to introduce a quasi-3D formulation for examining the buckling, bending and free vibration response of BDFG curved sandwich beams. The kinematics employed involves undetermined integral terms and gives only four unknowns functions. The governing equations are obtained utilizing Hamilton's principle and then are solved by Navier solution for the simply supported cases. An in-depth study of the impact of various parameters on the bending, buckling and free vibration of BDFG sandwich curved beams is presented.

## 2. Problem description

### 2.1. BDFG sandwich curved beams configuration and properties

In the presents work, a BDFG curved sandwich beam simply supported is analyzed as indicated in Fig.1

The BDFG curved sandwich beam is composed from three layers, the top and bottom layers have characteristics that vary in both directions while the core layer has isotropic characteristics.

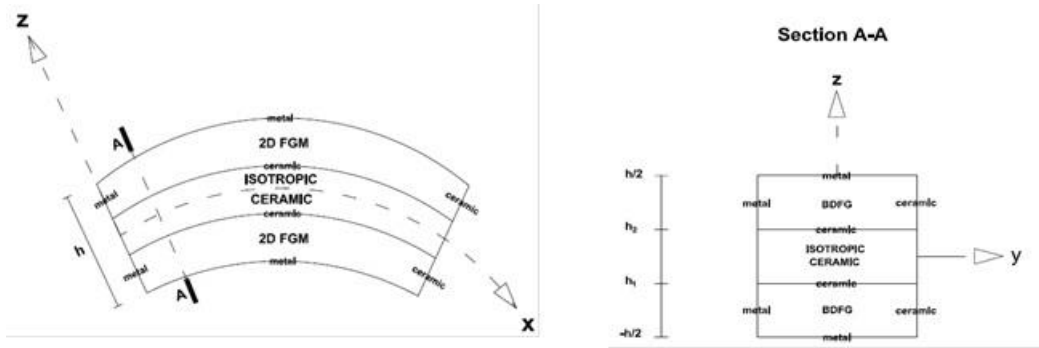


Fig 1: BDFG curved sandwich beam

The effective material properties for n-th layer, like the Young's modulus  $E^{(n)}$  and the mass density  $\rho^{(n)}$  are expressed as [30].

$$1. P^{(n)}(x, z) = (P_1 - P_2)V^{(n)}(z) + P_2$$

2. where  $P^{(n)}$  is the effective material property of FG of layer n.  $P_1$  and  $P_2$  are the properties of the top and bottom faces of layer 1, respectively, and vice versa for layer 3 depending on the volume fraction  $V^{(n)}$ , ( $n = 1, 2, 3$ ).

$$\begin{cases} V^{(1)}(z) = \left(\frac{z - h_0}{h_1 - h_0}\right)^{n_z} & \text{for } z \in [h_0, h_1] \\ V^{(2)}(z) = 1 & \text{for } z \in [h_1, h_2] \\ V^{(3)}(z) = \left(\frac{z - h_3}{h_2 - h_3}\right)^{n_z} & \text{for } z \in [h_2, h_3] \end{cases} \quad V(x) = \left(\frac{x}{L}\right)^{n_x} \quad (2)$$

Where  $V^{(n)}$  is the volume fraction of n-th layer and  $n_z, n_x$  is a parameter that denotes the power index and takes values greater than or equal to zero.

### 2.2. Kinematics and constitutive equations

The quasi-3D displacement field used in this work is:

$$u(x, y, z, t) = \left(1 + \frac{z}{R}\right)u_0(x, y, t) - z \frac{\partial w_0}{\partial x} + k_1 f(z) \int \theta(x, y, t) dx \quad (3a)$$

$$w(x, y, z, t) = w_0(x, y, t) + g(z)\theta \quad (3b)$$

with

$$f(z) = z \times \cosh\left(\frac{1}{2}\right) - h \times \sinh\left(\frac{z}{h}\right) \quad g(z) = \frac{1}{7} \frac{df(z)}{dz} \tag{4}$$

The kinematic relations can be obtained as follows:

$$\varepsilon_x = \varepsilon_x^0 + zk_x^b + f(z)k_x^s + g(z)\varepsilon_x^1, \quad \{\gamma_{xz}\} = f'(z)\{\gamma_{xz}^0\} + g(z)\{\gamma_{xz}^1\}, \quad \varepsilon_z = g'(z)\varepsilon_z^0 \tag{5a}$$

where

$$\{\varepsilon_x^0\} = \left\{ \frac{\partial u_0}{\partial x} + \frac{w_0}{R} \right\}, \quad \left\{ \begin{matrix} k_x^b \\ k_x^s \end{matrix} \right\} = \left\{ \begin{matrix} -\frac{\partial^2 w_0}{\partial x^2} \\ k_1 \theta \end{matrix} \right\}, \quad \{\varepsilon_x^1\} = \left\{ \frac{\theta}{R} \right\} \tag{5b}$$

$$\{\gamma_{xz}^0\} = \left\{ k_1 \int \theta dx \right\}, \quad \{\gamma_{xz}^1\} = \left\{ \frac{\partial \theta}{\partial x} \right\} \tag{5c}$$

$$\varepsilon_z^0 = \theta, \quad g'(z) = \frac{dg(z)}{dz} \tag{5d}$$

With the help of the Navier-type approach, the integrals used in Eq.(3a) can be stated as  $\int \theta dx = A' \frac{\partial \theta}{\partial x}$

$A'$  is a coefficient depending on the Navier solution, and is expressed as:

$$A' = -\frac{1}{\alpha^2}, \quad k_1 = -\alpha^2 \tag{6}$$

where  $\alpha$  defined in expression (19).

The constitutive relations are:

$$\left\{ \begin{matrix} \sigma_x \\ \sigma_z \\ \tau_{xz} \end{matrix} \right\} = \begin{bmatrix} C_{11} & C_{12} & 0 \\ C_{12} & C_{22} & 0 \\ 0 & 0 & C_{55} \end{bmatrix} \left\{ \begin{matrix} \varepsilon_x \\ \varepsilon_z \\ \gamma_{xz} \end{matrix} \right\} \tag{7}$$

For the quasi-3D solution used here, we have:

$$C_{11} = C_{22} = \frac{(1-\nu)E(x,z)}{(1-2\nu)(1+\nu)}, \tag{8a}$$

$$C_{12} = \frac{E(x,z)\nu}{(1-2\nu)(1+\nu)}, \tag{8b}$$

$$C_{55} = \frac{E(x,z)}{2(1+\nu)}. \tag{8c}$$

The Hamilton's principle is stated as follows:

$$0 = \int_0^t (\delta U - \delta V - \delta K) dt \tag{9}$$

The variation of strain energy  $\delta U$  is

$$\delta U = \int_A [\sigma_x \delta \varepsilon_x + \sigma_z \delta \varepsilon_z + \tau_{xz} \delta \gamma_{xz}] dV \tag{10a}$$

$$\int_0^L [N_x \delta \varepsilon_x^0 + N_z \delta \varepsilon_z^0 + M_x^b \delta k_x^b + M_x^s \delta k_x^s + Q_{xz} \delta \gamma_{xz}^0 + S_{xz} \delta \gamma_{xz}^1 + Q_x \delta \varepsilon_x^1] dx$$

Stress resultants N, M, Q, and S are defined by

$$\begin{Bmatrix} N_x \\ M_x^b \\ M_x^s \end{Bmatrix} = \sum_{n=1}^3 \int_{h_{n-1}}^{h_n} \sigma_x \begin{Bmatrix} 1 \\ z \\ f(z) \end{Bmatrix} dz \tag{10b}$$

$$N_z = \sum_{n=1}^3 \int_{h_{n-1}}^{h_n} \sigma_z g'(z) dz, S_{xz} = \sum_{n=1}^3 \int_{h_{n-1}}^{h_n} \tau_{xz} g(z) dz, Q_{xz}^s = \sum_{n=1}^3 \int_{h_{n-1}}^{h_n} \tau_{xz} f'(z) dz, Q_x = \sum_{n=1}^3 \int_{h_{n-1}}^{h_n} \sigma_x g(z) dz \tag{10c}$$

Where  $h_n$  and  $h_{n-1}$  are the top and bottom z-coordinates of the nth layer

The variation of work  $\delta V$  done by in-plane and transverse loads is given by:

$$\delta V = \int_0^L \left[ N \frac{\partial^2 w}{\partial x^2} \right] \delta w dx + \int_0^L q \delta w dx \tag{11}$$

The variation of kinetic energy  $\delta K$  of the plate can be expressed as

$$\delta K = \int \int_{x,z} [\dot{u} \delta \dot{u} + \dot{w} \delta \dot{w}] \rho(x, z) dx dz \tag{12}$$

$$= \int_x \{ I_0 \dot{u}_0 \delta \dot{u}_0 + I_1 \frac{\partial \dot{w}_0}{\partial x} \delta \dot{u}_0 - I_2 \frac{\partial \dot{\theta}}{\partial x} \delta \dot{u}_0 - I_1 \frac{\partial \dot{u}_0}{\partial x} \delta \dot{w}_0 + I_3 \frac{\partial \dot{w}_0}{\partial x} \frac{\partial \delta \dot{w}_0}{\partial x} - I_4 \frac{\partial \dot{\theta}}{\partial x} \frac{\partial \delta \dot{w}_0}{\partial x} + I_2 \frac{\partial \dot{u}_0}{\partial x} \frac{\partial \delta \dot{\theta}}{\partial x} - I_4 k_1 A' \frac{\partial \dot{w}_0}{\partial x} \frac{\partial \delta \dot{\theta}}{\partial x} + I_6 k_1 A' \frac{\partial \dot{\theta}}{\partial x} \frac{\partial \delta \dot{\theta}}{\partial x} - J_1 \dot{w}_0 \delta \dot{w}_0 - J_2 \dot{\theta} \delta \dot{w}_0 - J_2 \dot{w}_0 \delta \dot{\theta} - J_3 \dot{\theta} \delta \dot{\theta} \} dx$$

where dot-superscript convention indicates the differentiation with respect to the time variable  $t$ ;  $\rho(z)$  is the mass density given by Eq. (2); and  $(I_i, J_i)$  are mass inertias expressed by

$$(I_0, I_1, I_2) = \sum_{n=1}^3 \int_{h_{n-1}}^{h_n} \left[ \left(1 - \frac{z}{R}\right)^2, \left(1 - \frac{z}{R}\right)z, k_1 A' \left(1 - \frac{z}{R}\right) f(z) \right] \rho(x, z) dz \tag{13a}$$

$$(I_3, I_4, I_6) = \sum_{n=1}^3 \int_{h_{n-1}}^{h_n} \left( z^2, k_1 A' z f(z), (k_1 A')^2 f(z) \right) \rho(x, z) dz \tag{13b}$$

$$(J_1, J_2, J_3) = \sum_{n=1}^3 \int_{h_{n-1}}^{h_n} (1, f(z), g(z)^2) \rho(x, z) dz \tag{14a)c}$$

Replacing Eqs. (10), (11) and (12) into Eq. (9), the following can be derived:

$$\int_x \left( \frac{\partial N_x}{\partial x} - I_0 \ddot{u}_0 + I_1 \frac{\partial \ddot{w}_0}{\partial x} - I_2 \frac{\partial \ddot{\theta}}{\partial x} \right) \delta u_0 dx = 0 \tag{14b}$$

$$\int_x \left( \begin{aligned} &\frac{\partial^2 M_x^b}{\partial x^2} - \frac{N_x}{R} + q + \bar{N} \left( \frac{\partial^2 w_0}{\partial x^2} + g(z) \frac{\partial^2 \theta}{\partial x^2} \right) - I_0 \ddot{w}_0 \\ &- I_1 \frac{\partial \ddot{u}_0}{\partial x} + I_3 \frac{\partial^2 \ddot{w}_0}{\partial x^2} - I_4 \frac{\partial^2 \ddot{\theta}}{\partial x^2} - J_1 \ddot{w}_0 - J_2 \ddot{\theta} \end{aligned} \right) \delta w_0 dx = 0 \tag{14c}$$

$$\int_x \left( \begin{aligned} &-k_1 A' \frac{\partial^2 M_x^s}{\partial x^2} + \frac{W_0}{R} - N_z + k_1 A' \frac{\partial Q_{xz}^s}{\partial x} + \frac{\partial S_{xz}^s}{\partial x} + g(z)q + g(z)\bar{N} \left( \frac{\partial^2 w_0}{\partial x^2} + g(z) \frac{\partial^2 \theta}{\partial x^2} \right) \\ &+ I_2 \frac{\partial \ddot{u}_0}{\partial x} + I_6 (k_1 A')^2 \frac{\partial \ddot{\theta}}{\partial x} - I_4 \frac{\partial^2 \ddot{w}_0}{\partial x^2} - J_2 \ddot{w}_0 - J_3 \ddot{\theta} \end{aligned} \right) \delta \theta dx = 0$$

The stress resultants are obtained as:

$$\begin{Bmatrix} N_x \\ M_x^b \\ M_x^s \end{Bmatrix} = \begin{bmatrix} A & B & B^s \\ B & D & D^s \\ B^s & D^s & H^s \end{bmatrix} \begin{Bmatrix} \varepsilon_x^0 \\ k_x^b \\ k_x^s \end{Bmatrix} + \begin{bmatrix} L \\ L^a \\ E \end{bmatrix} \varepsilon_0^z, \quad \begin{Bmatrix} Q \\ S \end{Bmatrix} = \begin{bmatrix} F^s & X^s \\ X^s & A^s \end{bmatrix} \begin{Bmatrix} \gamma^0 \\ \gamma^1 \end{Bmatrix} \tag{15a}$$

$$N_z = R^a \varepsilon_z^0 + L \varepsilon_x^0 + L^a k_x^b + E k_x^s \tag{15b}$$

where

$$S = \{S_{xz}\}, Q = \{Q_{xz}\} \tag{15c}$$

$$\begin{Bmatrix} L \\ L^a \\ E \\ R^a \end{Bmatrix} = \sum_{n=1}^3 \int_{h_{n-1}}^{h_n} C_{12} \begin{Bmatrix} 1 \\ z \\ f(z) \\ g'(z) \end{Bmatrix} g'(z) dz \tag{15d}$$

$$\{A_{11}, B_{11}, D_{11}, B_{11}^s, D_{11}^s, H_{11}^s\} = \sum_{n=1}^3 \int_{h_{n-1}}^{h_n} C_{11} [1, z, z^2, f(z), zf(z), f^2(z)] dz \tag{15e}$$

$$\{E_{11}, F_{11}, K_{11}^s, K_{11}\} = \sum_{n=1}^3 \int_{h_{n-1}}^{h_n} C_{11} [g(z), zg(z), f(z)g(z), g^2(z)] dz \tag{15f}$$

$$\{E_{13}^s, j_{13}^s\} = \sum_{n=1}^3 \int_{h_{n-1}}^{h_n} C_{12} [g'(z), g'(z)g(z)] dz \tag{15j}$$

$$(F_{44}^s, X_{44}^s, A_{44}^s) = \sum_{n=1}^3 \int_{h_{n-1}}^{h_n} \left( \frac{E(x, z)}{2(1+\nu)} [f'^2(z), f'(z)g(z), g^2(z)] \right) dz \tag{15h}$$

Replacing Eq. (15) into Eq. (14), the equations of motion can be expressed in terms of displacements ( $u_0, w_0, \theta$ ) as:

$$\int_0^L \begin{bmatrix} A_{11}d_{11}u_0 + d_1A_{11}d_1u_0 + A_{11} \frac{d_1w_0}{R} + d_1A_{11} \frac{w_0}{R} - B_{11}d_{111}w_0 - d_1B_{11}d_{11}w_0 \\ + B_{11}^s k_1 A' d_{111}\theta + d_1 B_{11}^s k_1 A' d_{11}\theta + L d_1\theta + d_1 L\theta + E_{11} \frac{d_1\theta}{R} + d_1 E_{11} \frac{\theta}{R} \\ - I_0 \ddot{u}_0 + I_1 d_1 \ddot{w}_0 - I_2 d_1 \ddot{\theta} \end{bmatrix} \delta u_0 dx = 0 \tag{16a}$$

$$\int_0^L \begin{bmatrix} B_{11}d_{111}u_0 + d_{11}B_{11}d_1u_0 + 2B_{11} \frac{d_1w_0}{R} + d_{11}B_{11} \frac{w_0}{R} - D_{11}d_{1111}w_0 - d_{11}D_{11}d_{11}w_0 \\ + k_1 A' D_{11}^s d_{1111}\theta + k_1 A' d_{11} D_{11}^s d_{11}\theta + F_{11} \frac{d_{11}\theta}{R} + d_{11} F_{11} \frac{\theta}{R} - \frac{A_{11}}{R} d_1 u_0 - \frac{A_{11}}{R^2} w_0 \\ - k_1 A' \frac{B_{11}^s}{R} d_{11}\theta - \frac{E_{11}}{R^2} \theta - \frac{E_{13}^s}{R} \theta + L^a d_{11}\theta + q + \bar{N} (d_{11}w_0 + g(z)d_{11}\theta) \\ - I_0 \ddot{w}_0 - I_1 d_1 \ddot{u}_0 + I_3 d_{11} \ddot{w}_0 - I_4 d_{11} \ddot{\theta} - J_1 \ddot{w}_0 - J_2 \ddot{\theta} \end{bmatrix} \delta w_0 dx = 0 \tag{16b}$$

$$\int_0^L \begin{bmatrix} -k_1 A' \left( B_{11}^s d_{111}u_0 + d_{11} B_{11}^s d_1 u_0 + d_{11} B_{11}^s \frac{w_0}{R} + B_{11}^s \frac{d_{11}w_0}{R} \right) \\ + k_1 A' \left( D_{11}^s d_{1111}w_0 + d_{11} D_{11}^s d_{11}w_0 \right) - (k_1 A')^2 \left( H_{11}^s d_{1111}\theta + d_{11} H_{11}^s d_{11}\theta \right) \\ - L d_1 u_0 + L^a d_{11} w_0 - 2k_1 A' E d_{11}\theta - k_1 A' \left( d_{11} K_{11}^s \frac{\theta}{R} + K_{11}^s \frac{d_{11}\theta}{R} \right) \\ - \frac{1}{R} \left( E_{11} d_1 u_0 + E_{11} \frac{w_0}{R} - F_{11} d_{11} w_0 + k_1 A' K_{11}^s d_{11}\theta + A_{44}^s \frac{\theta}{R} + 2j_{13}^s \theta \right) \\ - E_{13}^s \frac{w_0}{R} - R^a \theta + \left( A_{44}^s + (k_1 A')^2 F_{44}^s + 2k_1 A' X_{44}^s \right) d_{11}\theta \\ + \left( d_1 A_{44}^s + (k_1 A')^2 d_1 F_{44}^s + 2k_1 A' d_1 X_{44}^s \right) d_1 \theta + qg(z) \\ + g(z) \bar{N} (d_{11}w_0 + g(z)d_{11}\theta) + I_2 d_1 \ddot{u}_0 + I_6 (k_1 A')^2 d_1 \ddot{\theta} - I_4 d_{11} \ddot{w}_0 - J_2 \ddot{w}_0 - J_3 \ddot{\theta} \end{bmatrix} \delta \theta dx = 0 \tag{16c}$$

### 3. Solution for BDFG curved sandwich beams simply rested

The following representation is considered the solution for the case of our problem:

$$\begin{Bmatrix} u_0 \\ w_0 \\ \theta \end{Bmatrix} = \sum_{m=1}^{\infty} \begin{Bmatrix} U_m e^{i\omega t} \frac{\partial X(x)}{\partial x} \\ W_m e^{i\omega t} X(x) \\ X_m e^{i\omega t} X(x) \end{Bmatrix} \quad (17)$$

For simply supported case:

$$X(x) = \sin(\alpha x) \quad (18)$$

where  $\omega$  is the frequency of the beam,  $\sqrt{i} = -1$  the imaginary unit.

with

$$\alpha = m\pi / a \quad (19)$$

Replacing Eq. (17) into Eq. (16), one will have:

$$\begin{bmatrix} a_{11} & a_{12} & a_{13} \\ a_{21} & a_{22} & a_{23} \\ a_{31} & a_{32} & a_{33} \end{bmatrix} \begin{Bmatrix} U_m \\ W_m \\ X_m \end{Bmatrix} = \begin{Bmatrix} 0 \\ 0 \\ 0 \end{Bmatrix} \quad (20)$$

where

$$\begin{aligned} a_{11} &= \int_x \left[ A_{11} d_{111} X + d_1 A_{11} d_{11} X - I_0 d_1 X \omega^2 \right] d_1 X dx \\ a_{12} &= \int_x \left[ A_{11} \frac{d_1 X}{R} + d_1 A_{11} \frac{X}{R} - B_{11} d_{111} X - d_1 B_{11} d_{11} X + I_1 d_1 X \omega^2 \right] d_1 X dx \\ a_{13} &= \int_x \left[ k_1 A' B_{11}^s d_{111} X + k_1 A' d_1 B_{11}^s d_{11} X + E_{11} \frac{d_1 X}{R} + d_1 E_{11} \frac{X}{R} \right. \\ &\quad \left. + L d_1 X + d_1 L X + k_1 A' I_2 d_1 X \omega^2 \right] d_1 X dx \end{aligned}$$

$$\begin{aligned}
 a_{21} &= \int_x \left[ B_{11} d_{1111} X + d_{11} B_{11} d_{11} X - A_{11} \frac{d_{11} X}{R} - I_1 d_{11} X \omega^2 \right] X dx \\
 a_{21} &= \int_x \left[ B_{11} \frac{d_{11} X}{R} + d_{11} A_{11} \frac{X}{R} - A_{11} \frac{X}{R^2} + B_{11} \frac{d_{11} X}{R} - D_{11} d_{1111} X - d_{11} D_{11} d_{11} X \right. \\
 &\quad \left. + I_0 X \omega^2 + I_3 d_{11} X \omega^2 - J_1 X \omega^2 \right] X dx \\
 a_{23} &= \int_x \left[ F_{11} \frac{d_{11} X}{R} + d_{11} F_{11} \frac{X}{R} + k_1 A' D_{11}^s d_{1111} X + k_1 A' d_{11} D_{11}^s d_{11} X + L^a d_{11} X + d_{11} L^a X \right. \\
 &\quad \left. - k_1 A' B_{11}^s \frac{d_{11} X}{R} - E_{11} \frac{X}{R^2} - E_{13} \frac{X}{R} + k_1 A' J_2 d_{11} X \omega^2 - I_4 k_1 A' d_{11} X \omega^2 - J_2 X \omega^2 \right] X dx \\
 a_{31} &= \int_x \left[ k_1 A' B_{11}^s d_{1111} X + k_1 A' d_{11} B_{11}^s d_{11} X - E_{11} \frac{d_{11} X}{R} - k_1 A' I_2 d_{11} X \omega^2 \right] X dx \\
 a_{32} &= \int_x \left[ k_1 A' D_{11}^s d_{1111} X + k_1 A' d_{11} D_{11}^s d_{11} X - k_1 A' B_{11}^s \frac{d_{11} X}{R} - E_{11} \frac{X}{R^2} \right. \\
 &\quad \left. + F_{11} \frac{d_{11} X}{R} - E_{13} \frac{X}{R} + k_1 A' J_2 d_{11} X \omega^2 - k_1 A' I_4 d_{11} X \omega^2 + J_2 X \omega^2 \right] X dx \\
 a_{33} &= \int_x \left[ - (k_1 A')^2 H_{11}^s d_{1111} X - (k_1 A')^2 d_{11} H_{11}^s d_{11} X - 2k_1 A' E d_{11} X - k_1 A' d_{11} K_{11}^s \frac{X}{R} \right. \\
 &\quad - R^a X + (A_{44}^s + (k_1 A')^2 F_{44}^s + 2k_1 A' X_{44}^s) d_{11} X \\
 &\quad + (d_{11} A_{44}^s + (k_1 A')^2 d_{11} F_{44}^s + 2k_1 A' d_{11} X_{44}^s) d_{11} X \\
 &\quad \left. - k_1 A' K_{11}^s \frac{d_{11} X}{R} - K_{11} \frac{X}{R^2} - 2J_{13}^s \frac{X}{R} - J_3 X \omega^2 + (k_1 A')^2 I_6 d_{11} X \omega^2 \right] X dx
 \end{aligned}
 \tag{21}$$

And

$$\begin{aligned}
 F_1 &= 0 \\
 F_2 &= - \int_x [q_m X] dx \\
 F_3 &= \int_x [q_m X g(z)] dx
 \end{aligned}
 \tag{22}$$

The transverse load q is also expanded in the double-Fourier sine series as

$$q(x) = \sum_{m=1}^{\infty} q_m \sin(\alpha x)
 \tag{23}$$

For the case of a sinusoidally distributed load, it is

$$m = 1 \text{ and } q_m = q_0 \quad (24)$$

where  $q_0$  intensity of the load at the beam center. For the case of a uniformly distributed load (UDL), it is:

$$q_m = \frac{4q_0}{m\pi} \quad m = 1, 3, 5, \dots, \infty \quad (25)$$

#### 4. Numerical results and discussion

In this part of paper, various examples will be presented and discussed relating to bending, free vibration and buckling of BDFG curved sandwich beams. Therefore, this section will be divided into three parts.

In the following calculations, a BDFG curved sandwich beam with the following characteristics is used:

Ceramic (Alumina,  $Al_2O_3$ )  $E_c = 380 \text{ GPa}$

Metal (Aluminium,  $Al$ )  $E_m = 70 \text{ GPa}$

The following forms are employed in the different representation of results:

$$\bar{u} = \frac{100E_m h^3}{q_0 L^4} u \left( 0, -\frac{h}{2} \right) \quad \bar{w} = \frac{100E_m h^3}{q_0 L^4} w \left( \frac{L}{2}, 0 \right) \quad \bar{\sigma}_{xx} = \frac{h}{q_0 L} \sigma_{xx} \left( \frac{L}{2}, \frac{h}{2} \right) \quad \bar{\omega} = \frac{\omega L^2}{h} \sqrt{\frac{\rho_m}{E_m}}$$

$$N_{cr} = N_0 \frac{12L^2}{E_m h^3}$$

##### 4.1. Bending analysis

This part of the paper is reserved for the results of the present formulation for the static bending of simply supported BDFG curved sandwich beams. First for all, results computing with the present formulation are compared with those from different theories presented in scientific publications dealing with the same problem. In this regard, a verification is carried out between the results of the present quasi-3D formulation with three unknowns functions and those of Sayyad and Ghugal [9] using quasi-3D sinusoidal shear deformation theory, Avhad and Sayyad[14] based on fifth-order shear and normal deformation theory (FOSNDT) and Draiche et al.[31] employing a quasi-3D shear deformation theory with four unknowns functions.

We list in tables 1-3, a comparison between non-dimensional axial displacement  $\bar{u}$ , non-dimensional deflection and non-dimensional axial stress  $\bar{\sigma}_{xx}$  of FG sandwich curved beams simply supported under uniform loading respectively. One can noted that there is a good concordance between all results.

In table 4, results of the current formulation in term of  $\bar{u}$ ,  $\bar{w}$  and  $\bar{\sigma}_{xx}$  for different configuration of simply supported BDFG curved sandwich beams are reported. The beams are expected to be submitted to a sinusoidally distributed load. In addition, the results are presented for different grading indexes and different values of radius of curvature (R/h).

After examining the obtained results, the following conclusions can be drawn:

- Increasing the values of the R/h ratio results in a reduction of the values of the axial displacement, regardless of the type of sandwich, the material composition of the beam (variation of  $n_x$  and  $n_z$ ) and the slenderness ratio (L/h) used,

- The deflection values are not affected by the variation of the radius of curvature values. The axial stresses are only slightly affected by this variation, where a very slight increase can be noticed,
- For the same values of L/h and R/h ratios as well as the material composition of the beam, the lowest values of displacements and stresses are obtained for the sandwich type (1-2-1). This result can be justified by the fact that the thickness of the core layer is two (02) times thicker than the other layers. Knowing that this layer is isotropic composed by the ceramic, therefore it is more rigid which favors the reduction of the parameter's response of the beam,
- A comparison between displacement ( $\bar{u}$ ,  $\bar{w}$ ) and stress ( $\bar{\sigma}_{xx}$ ) values reveals that the isotropic beam ( $n_x=n_z=0$ ) shows lower results compared to the FG beams.

The variation of the nondimensional axial displacement  $\bar{u}$ , the nondimensional deflexion  $\bar{w}$  and the nondimensional axial stress  $\bar{\sigma}_{xx}$  across the thickness of BDFG curved sandwich beams submitted to a sinusoidally distributed load is represented respectively in Fig.2 a-c. Three kind of beams are studied, isotropic sandwich beam ( $n_x=n_z=0$ ), transversally functionally graded sandwich beam ( $n_z=1, n_x=0$ ) and BDFG sandwich beam ( $n_z=1, n_x=1$ ).

**Table 1: Verification of  $\bar{u}$  for a transverselyFG sandwich curved beams under uniform loading ( $n_x=0$ )**

R/h	n <sub>z</sub>	Theory	L/h=5			L/h=20		
			2-1-2	1-1-1	1-2-1	2-1-2	1-1-1	1-2-1
5	0	Ref[9]	-	1.8244	-	-	-	-
		Ref[14]	1.9111	1.9111	1.9111	3.5597	3.5593	3.5597
		Ref[31]	1.8299	1.8299	1.8299	3.5644	3.5644	3.5645
		Present	1.9098	1.9098	1.9098	3.5657	3.5657	3.5657
	1	Ref[9]	-	3.6707	-	-	-	-
		Ref[14]	4.1660	3.7665	3.2614	8.0805	7.9353	6.2672
		Ref[31]	4.0731	3.6801	3.1704	8.1032	7.3111	6.2776
		Present	4.1456	3.7532	3.2481	8.0919	7.3026	6.2737
	5	Ref[9]	-	6.6188	-	-	-	-
		Ref[14]	7.9700	6.7387	5.1209	15.6414	13.2728	10.0641
		Ref[31]	7.8107	6.6392	5.0226	15.7019	13.3390	10.0486
		Present	7.7943	6.6266	5.0509	15.6273	13.2759	10.0155
10	0	Ref[9]	-	1.3995	-	-	-	-
		Ref[14]	1.4856	1.4856	1.4856	1.9888	1.9888	1.9888
		Ref[31]	1.4033	1.4033	1.4033	1.9901	1.9901	1.9901
		Present	1.4836	1.4836	1.4836	1.9913	1.9913	1.9913
	1	Ref[9]	-	2.8300	-	-	-	-
		Ref[14]	3.2378	2.9276	2.5352	4.5168	4.0733	3.5025
		Ref[31]	3.1402	2.8365	2.4419	4.5247	4.0823	3.5053
		Present	3.2184	2.9139	2.5219	4.5190	4.0782	3.5036
	5	Ref[9]	-	5.1148	-	-	-	-
		Ref[14]	6.1938	5.2376	3.9257	8.7490	7.4235	5.6309
		Ref[31]	6.0340	5.1290	3.8777	8.7679	7.4489	5.6111
		Present	6.0500	5.1437	3.9209	8.7271	7.4139	5.5932
20	0	Ref[9]	-	1.1682	-	-	-	-
		Ref[14]	1.2539	1.2539	1.2539	1.1333	1.1333	1.1333
		Ref[31]	1.1710	1.1710	1.1710	1.1334	1.1334	1.1334
		Present	1.2516	1.2516	1.2516	1.1346	1.1346	1.1346
	1	Ref[9]	-	2.3726	-	-	-	-
		Ref[14]	2.7320	2.4706	2.1397	2.5746	2.3217	1.9962
		Ref[31]	2.6325	2.3774	2.0456	2.5774	2.3253	1.9966
		Present	2.7139	2.4571	2.1267	2.5747	2.3236	1.9962
	5	Ref[9]	-	4.2963	-	-	-	-
		Ref[14]	5.2255	4.4193	3.3597	4.9886	4.2327	3.2112
		Ref[31]	5.0671	4.3071	3.2546	4.9948	4.2434	3.1964
		Present	5.1008	4.3367	3.3060	4.9722	4.2240	3.1867

**Table 2: Verification of  $W$  for a transverselyFG sandwich curved beams under uniform loading ( $n_x=0$ )**

$R/h$	$n_z$	Theory	$L/h=5$			$L/h=20$		
			2-1-2	1-1-1	1-2-1	2-1-2	1-1-1	1-2-1
5	0	Ref[9]	–	3.1294	–	–	–	–
		Ref[14]	3.1775	3.1775	3.1775	2.8551	2.8551	2.8551
		Ref[31]	3.1394	3.1394	3.1394	2.8944	2.8944	2.8945
		Present	3.1814	3.1814	3.1814	2.8970	2.8970	2.8970
	1	Ref[9]	–	6.1913	–	–	–	–
		Ref[14]	6.9461	6.2763	5.4307	6.5667	5.6738	5.0931
		Ref[31]	6.8665	6.2092	5.3605	6.5791	5.9359	5.0970
		Present	6.8889	6.2377	5.4003	6.5312	5.9332	5.0972
	5	Ref[9]	–	11.0770	–	–	–	–
		Ref[14]	13.3090	11.2480	8.5579	12.7110	8.5781	8.5781
		Ref[31]	13.0790	11.1160	8.4264	12.7480	10.8290	8.1583
		Present	12.9294	10.9910	8.3819	12.6973	10.7866	8.1375
10	0	Ref[9]	–	3.1295	–	–	–	–
		Ref[14]	3.1775	3.1775	3.1775	2.8570	2.8570	2.8570
		Ref[31]	3.1396	3.1396	3.1396	2.8946	2.8946	2.8946
		Present	3.1816	3.1816	3.1816	2.8971	2.8971	2.8971
	1	Ref[9]	–	6.1916	–	–	–	–
		Ref[14]	6.9461	6.2763	5.4307	6.5667	5.6612	5.0931
		Ref[32]	6.8668	6.2094	5.3607	6.5795	5.9362	5.0973
		Present	6.8891	6.2378	5.4004	6.5748	5.9335	5.0974
	5	Ref[9]	–	11.0780	–	–	–	–
		Ref[14]	13.3090	11.2480	8.5579	12.7110	8.5601	8.5601
		Ref[31]	13.0800	11.1160	8.4266	12.7480	10.8300	8.1586
		Present	12.9297	10.9912	8.3821	12.6979	10.7872	8.1378
20	0	Ref[9]	–	3.1295	–	–	–	–
		Ref[14]	3.1775	3.1775	3.1775	2.8928	2.8928	2.8928
		Ref[31]	3.1396	3.1396	3.1396	2.8946	2.8946	2.8946
		Present	3.1816	3.1816	3.1816	2.8971	2.8971	2.8971
	1	Ref[9]	–	6.1916	–	–	–	–
		Ref[14]	6.9461	6.2763	5.4307	6.5667	5.6520	5.0931
		Ref[31]	6.8668	6.2094	5.3607	6.5796	5.9363	5.0974
		Present	6.8891	6.2379	5.4004	6.5749	5.9335	5.0975
	5	Ref[9]	–	11.0780	–	–	–	–
		Ref[14]	13.3090	11.2480	8.5579	12.7110	8.5457	8.1799
		Ref[31]	13.0800	11.1170	8.4267	12.7480	10.8300	8.1588
		Present	12.9298	10.9912	8.3821	12.6981	10.7873	8.1379

Fig.2-a shows that, for all beams, the variation of the axial displacement is linear through the thickness and the highest values are obtained for the BDFG sandwich beam. The same observation is made for figure 2-b. However, the variation of the deflection is not linear but presents a certain curvature. This is due to the quasi-3D nature of the present formulation which naturally takes the effect of thickness stretching. From the Fig.2-c, it can be seen that the variation of the axial stress is linear for the case of isotropic sandwich beam. But for the other beams, the variation is parabolic due to the variation of material composition of the skins. In addition, the maximum axial stress is observed for the sandwich curved beam with transversally functionally graded skins ( $n_z=1, n_x=0$ ).

In Fig.3-a-b the effect of radius of curvature ( $R/h$ ) and slenderness ratio ( $L/h$ ) on the nondimensional axial displacement and nondimensional deflection is represented respectively. After examining the obtained results, it should be noted that the radius curvature affects greatly the axial displacement while the deflection is insensitive to this parameter. Besides, the slenderness ratio affects slightly the deflection where a slight decrease is observed with the increase of this ratio. As for the axial displacement, an increase is noticed with the increase of the ( $L/h$ ) ratio. This increase becomes more notable with the decrease of radius of curvature ( $R/h$ ).

#### 4.2. Buckling analysis

At this stage of paper, numerical results are presented for the buckling of a BDFG sandwich curved beam simply supported. First, to confirm the precision of the current formulation, a numerical verification is performed as is reported in table 5.

In this table, critical buckling loads computed with the quasi-3D solution for FG straight sandwich beams ( $R/h=\infty$ ) are compared with those of Nguyen et al.[32] using a 2D HSDT analytical formulation and Vo et al.[33] employing FE model based on a refined HSDT. The verification is made for four (04) different configurations of

sandwich beams. Here again, on can be noted that the present formulation provides excellent agreement with the cited solutions.

**Table 3: Verification of  $\sigma_{xx}$  for a transverselyFG sandwich curved beams under uniform loading ( $n_x=0$ )**

R/h	n <sub>z</sub>	Theory	L/h=5			L/h=20		
			2-1-2	1-1-1	1-2-1	2-1-2	1-1-1	1-2-1
5	0	Ref[9]	–	3.8221	–	–	–	–
		Ref[14]	3.7557	3.7557	3.7556	14.8450	14.8450	14.8450
		Ref[31]	3.8318	3.8318	3.8318	15.1520	15.1520	15.1520
		Present	3.6083	3.6083	3.6083	13.3780	13.3780	13.3780
	1	Ref[9]	–	1.4449	–	–	–	–
		Ref[14]	1.5801	1.5068	1.2301	6.2374	6.1237	4.8387
		Ref[31]	1.6029	1.4466	1.2428	6.3691	5.7451	4.9305
		Present	1.5373	1.3859	1.1876	5.6312	5.0777	4.3550
	5	Ref[9]	–	2.6274	–	–	–	–
		Ref[14]	3.0234	2.5838	1.8933	12.0630	10.2648	7.4370
		Ref[31]	3.1004	2.6348	1.9867	12.3640	10.5024	7.9059
		Present	2.9989	2.5495	1.9170	11.9758	9.3223	7.0036
10	0	Ref[9]	–	3.8402	–	–	–	–
		Ref[14]	3.7557	3.7557	3.7556	14.8450	14.8450	15.1670
		Ref[31]	3.8134	3.8134	3.8134	15.0700	15.0700	15.0700
		Present	3.6284	3.6284	3.6284	13.4593	13.4593	13.4593
	1	Ref[9]	–	1.4526	–	–	–	–
		Ref[14]	1.5801	1.5068	1.2301	6.2374	6.1237	4.9527
		Ref[31]	1.5938	1.4385	1.2360	6.3287	5.7089	4.9001
		Present	1.5443	1.3924	1.1934	5.6698	5.1125	4.3846
	5	Ref[9]	–	2.6424	–	–	–	–
		Ref[14]	3.0234	2.5838	1.8933	12.0630	10.2640	7.6693
		Ref[31]	3.0817	2.6189	1.9750	12.2800	10.4310	7.8532
		Present	3.0099	2.5588	1.9247	11.0518	9.3872	7.0526
20	0	Ref[9]	–	3.8492	–	–	–	–
		Ref[14]	3.7557	3.7557	3.7556	14.8450	14.8450	15.1670
		Ref[31]	3.8042	3.8042	3.8042	15.0290	15.0290	15.0290
		Present	3.6384	3.6384	3.6384	13.5002	13.5002	13.5002
	1	Ref[9]	–	1.4564	–	–	–	–
		Ref[14]	1.5801	1.5068	1.2301	6.2374	6.1237	4.9527
		Ref[31]	1.5893	1.4344	1.2326	6.3085	5.6908	4.8848
		Present	1.5478	1.3956	1.1962	5.6892	5.1299	4.3994
	5	Ref[9]	–	2.6499	–	–	–	–
		Ref[14]	3.0234	2.5838	1.8933	12.0630	10.2640	7.6693
		Ref[31]	3.0724	2.6109	1.9691	12.2390	10.3960	7.8268
		Present	3.0154	2.5635	1.9285	11.0900	9.4198	7.0772

Figure 4 illustrates the relationship between nondimensional critical buckling load and the slenderness ratio (L/h) for three values of radius of curvature (R/h). The nondimensional critical buckling load increases as (L/h) ratio increases. Nonetheless, this increase is not as large as shown in the figure. For L/h=5 we have  $\bar{N}_{cr} = 15.68$  and for L/h=20,  $\bar{N}_{cr} = 16.6$ . However, as it can be seen, the radius of curvature (R/h) has no effect on  $\bar{N}_{cr}$ .

Figures 5 and 6 display the nondimensional critical buckling load as a function of the grading indexes n<sub>z</sub> and n<sub>x</sub> respectively. These results are obtained for a curved BDFG sandwich beam (1-1-1) and for three values of (L/h) ratio. These figures show that the same behavior is observed for the variation of the two grading indexes. This means that the increase in these indexes reduce substantially the nondimensional critical buckling load. This can be explained by the fact that increasing the n<sub>x</sub> and n<sub>z</sub> indexes leads to an increase in the amount of metal in the beam, which consequently becomes more flexible, thus reducing the critical buckling loads.

### 4.3. Free vibration analysis

The results on the current model for the case of the free vibration of the BDFG curved sandwich beams are presented here. In order to assess the performance of the present solution, it is important to validate in the free vibration analysis. For that, a comparison of the fundamental natural frequencies is performed in tables 6 and 7. It can be seen that the current results are in good agreement with the solutions of Refs [32, 33], so the accuracy of the current model is confirmed.

Figure 07 displays the variation of the nondimensional fundamental natural frequency with L/h ratio for three values of radius of curvature (R/h). Increasing the L/h ratio leads to a reduction in fundamental natural frequency. This reduction is much more pronounced for beams with low R/h ratio. When the latter ratio increases, i.e. for straight beams, the effect of the L/h ratio on the frequencies is minimal.

Figures 8 and 9 show, respectively, the variation of the nondimensional fundamental natural frequency according to nz and nx indexes. For both figures, the data indicate that the frequency diminish with increasing the indexes. Also, it is observed that the increase of L/h ratio leads to reduction of the frequency. This result is logical since the increase of the mentioned ratio leads to thin beams and therefore more flexible with low frequencies and high vibration periods.

**Table 4: response of a BDFG sandwich curved beam simply supported under sinusoidally distributed load**

R/h	n <sub>z</sub> ,n <sub>x</sub>		L/h=5			L/h=20		
			2-1-2	1-1-1	1-2-1	2-1-2	1-1-1	1-2-1
5	0,0	$\bar{u}$	1.4761	1.4761	1.4761	2.7937	2.7937	2.7937
		$\bar{w}$	2.5150	2.5150	2.5150	2.2845	2.2845	2.2845
		$\bar{\sigma}_{xx}$	2.9740	2.9740	2.9740	10.8566	10.8566	10.8566
	1,0	$\bar{u}$	3.2138	2.9090	2.5163	6.3405	5.7219	4.9157
		$\bar{w}$	5.4399	4.9260	4.2653	5.1840	4.6783	4.0192
		$\bar{\sigma}_{xx}$	1.2586	1.1352	0.9737	4.5722	4.1227	3.5357
	1,1	$\bar{u}$	4.5747	4.2584	3.8243	8.9421	8.3088	7.4247
		$\bar{w}$	7.7549	7.2206	6.4890	7.3113	6.7935	6.0708
		$\bar{\sigma}_{xx}$	1.7695	1.6438	1.4674	6.4337	5.9754	5.3337
	2,1	$\bar{u}$	5.6921	5.1901	4.4844	11.2383	10.2344	8.7892
		$\bar{w}$	9.6351	8.7863	7.5979	9.1885	8.3677	7.1862
		$\bar{\sigma}_{xx}$	2.2292	2.0304	1.7418	8.1065	7.3795	6.3270
10	0,0	$\bar{u}$	1.1421	1.1421	1.1421	1.5591	1.5591	1.5591
		$\bar{w}$	2.5152	2.5152	2.5152	2.2846	2.2846	2.2846
		$\bar{\sigma}_{xx}$	2.9903	2.9903	2.9903	10.9226	10.9226	10.9226
	1,0	$\bar{u}$	2.4871	2.2512	1.9472	3.5384	3.1933	2.7433
		$\bar{w}$	5.4401	4.9261	4.2655	5.1842	4.6785	4.0194
		$\bar{\sigma}_{xx}$	1.2642	1.1403	0.9783	4.6033	4.1507	3.5595
	1,1	$\bar{u}$	3.5401	3.2953	2.9593	4.9903	4.6369	4.1435
		$\bar{w}$	7.7551	7.2208	6.4892	7.3116	6.7939	6.0710
		$\bar{\sigma}_{xx}$	1.7779	1.6517	1.4747	6.4766	6.0152	5.3691
	2,1	$\bar{u}$	4.4051	4.0165	3.4703	6.2718	5.7116	4.9050
		$\bar{w}$	9.6353	8.7865	7.5981	9.1890	8.3681	7.1865
		$\bar{\sigma}_{xx}$	2.2391	2.0395	1.7499	8.1613	7.4295	6.3697
20	0,0	$\bar{u}$	0.9604	0.9604	0.9604	0.8873	0.8873	0.8873
		$\bar{w}$	2.5152	2.5152	2.5152	2.2846	2.2846	2.2846
		$\bar{\sigma}_{xx}$	2.9984	2.9984	2.9984	10.9557	10.9557	10.9557
	1,0	$\bar{u}$	2.0917	1.8932	1.6376	2.0137	1.8172	1.5612
		$\bar{w}$	5.4401	4.9262	4.2655	5.1843	4.6786	4.0194
		$\bar{\sigma}_{xx}$	1.2670	1.1429	0.9806	4.6189	4.1648	3.5715
	1,1	$\bar{u}$	2.9771	2.7712	2.4886	2.8399	2.6388	2.3580
		$\bar{w}$	7.7552	7.2209	6.4893	7.3117	6.7939	6.0711
		$\bar{\sigma}_{xx}$	1.7821	1.6556	1.4783	6.4982	6.0352	5.3868
	2,1	$\bar{u}$	3.7047	3.3779	2.9184	3.5692	3.2504	2.7914
		$\bar{w}$	9.6354	8.7866	7.5982	9.1891	8.3682	7.1866
		$\bar{\sigma}_{xx}$	2.2441	2.0440	1.7540	8.1888	7.4546	6.3912

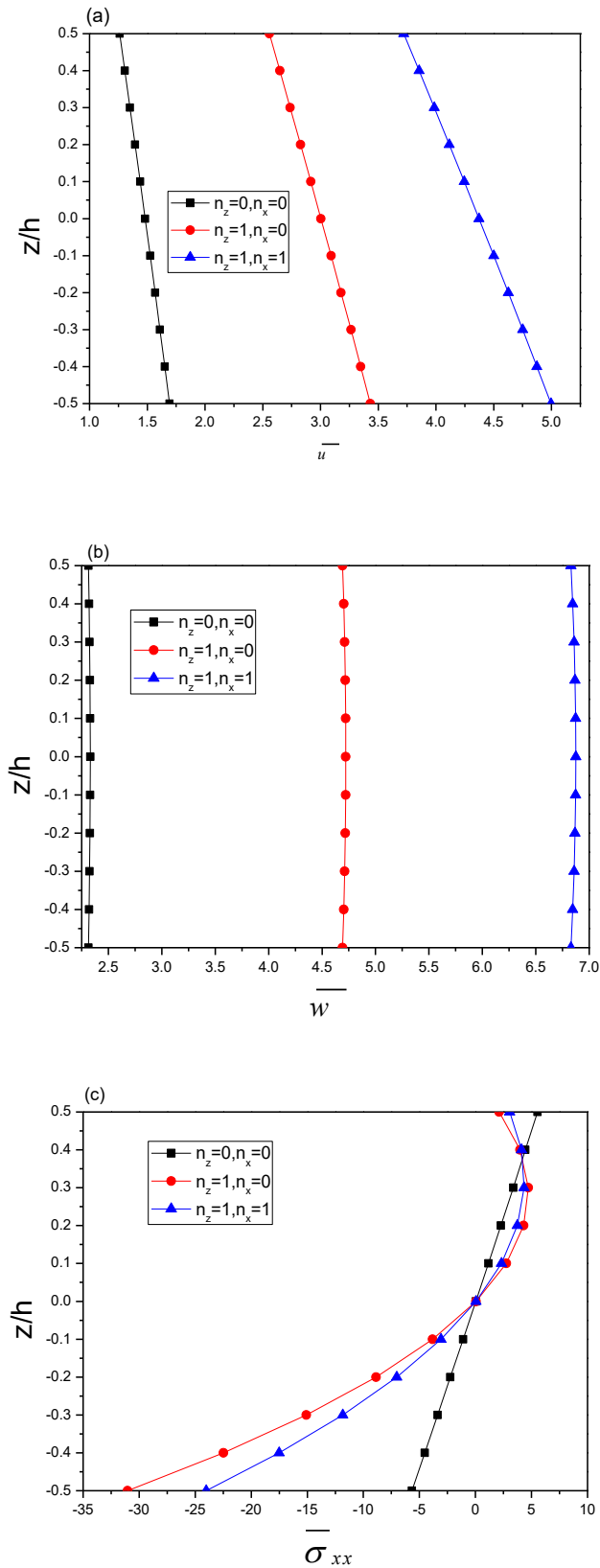


Figure 02: Response of curved sandwich under sinusoidally distributed load (a) variation of  $\bar{u}$  across the thickness (b) variation of  $\bar{w}$  across the thickness (c) variation of  $\bar{\sigma}_{xx}$  across the thickness ((1-1-1),  $R/h=5, L/h=10$ )

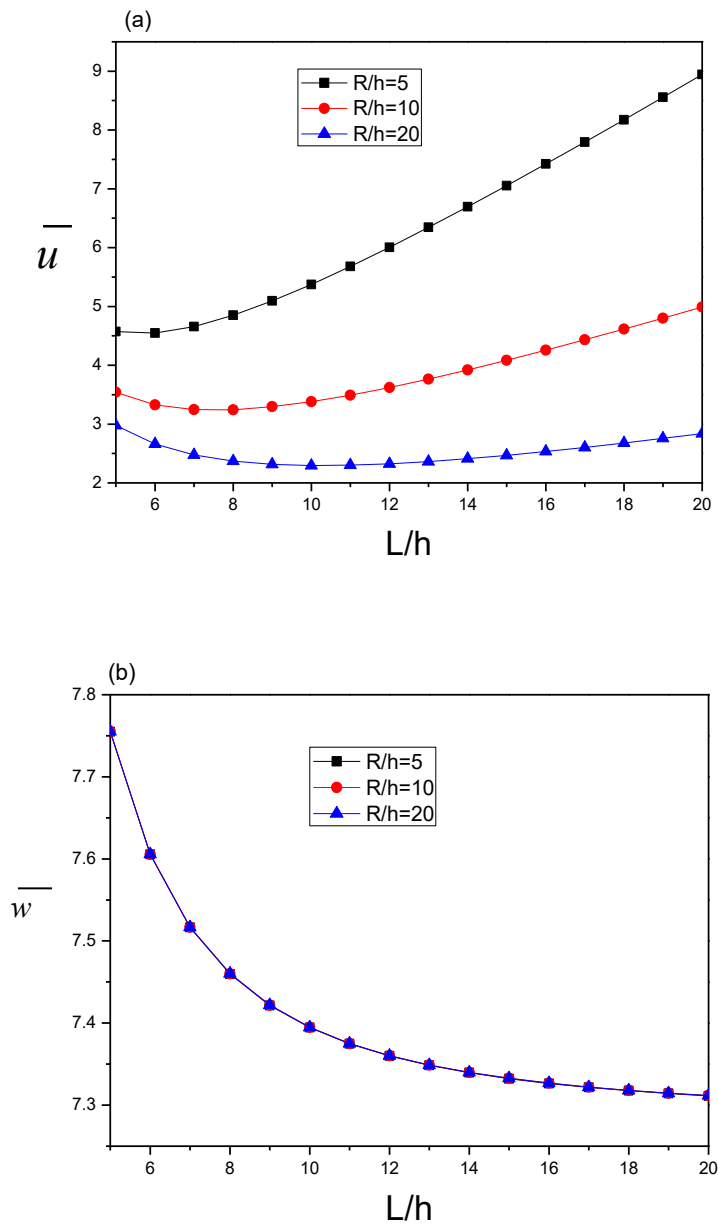


Figure 03: Effect of  $(L/h)$  on (a) axial displacement (b) deflection ((2-1-2),  $n_x=n_z=1$ )

**Table 5: Verification of  $\bar{N}_{cr}$  (nx=0, L/h=5, R/h=infinity)**

$n_z$	Theory	1-0-1	2-1-2	1-1-1	1-2-1
0	Present	48.3400	48.3400	48.3400	48.3400
	Nguyen et al. [32]	48.5964	48.5964	48.5964	48.5964
	Vo et al. [33]	48.5959	48.5959	48.5959	48.5959
0.5	Present	27.8462	30.0134	31.8418	34.6845
	Nguyen et al. [32]	27.8380	30.0146	31.8650	34.7546
	Vo et al. [33]	27.8574	30.0301	31.8784	34.7653
1	Present	19.7718	22.3499	24.6815	28.5044
	Nguyen et al. [32]	19.6541	22.2121	24.5602	28.4440
	Vo et al. [33]	19.6525	22.2108	24.5596	28.4447
2	Present	13.7464	16.1519	18.6023	22.9774
	Nguyen et al. [32]	13.5820	15.9167	18.3596	22.7859
	Vo et al. [33]	13.5801	15.9152	18.3587	22.7863
5	Present	10.2455	11.9143	14.0154	18.3745
	Nguyen et al. [32]	10.1460	11.6697	13.7226	18.0915
	Vo et al. [33]	10.1460	11.6676	13.7212	18.0914

**Table 6: Verification of  $\bar{\omega}$  (nx=0, L/h=5, R/h=infinity)**

$n_z$	Theory	1-0-1	2-1-2	1-1-1	1-2-1
0	Present	5.2696	5.2696	5.2696	5.2696
	Nguyen et al. [32]	5.1528	5.1528	5.1528	5.1528
	Vo et al. [33]	5.1528	5.1528	5.1528	5.1528
0.5	Present	4.2052	4.3202	4.4194	4.5739
	Nguyen et al. [32]	4.1254	4.2340	4.3294	4.4791
	Vo et al. [33]	4.1268	4.2351	4.3303	4.4798
1	Present	3.6402	3.8069	3.9581	4.1989
	Nguyen et al. [32]	3.5736	3.7298	3.8756	4.1105
	Vo et al. [33]	3.5735	3.7298	3.8755	4.1105
2	Present	3.1229	3.3075	3.4975	3.8187
	Nguyen et al. [32]	3.0682	3.2366	3.4190	3.7334
	Vo et al. [33]	3.0680	3.2365	3.4190	3.7334
5	Present	2.7799	2.9063	3.0919	3.4599
	Nguyen et al. [32]	2.7450	2.8441	3.0182	3.3771
	Vo et al. [33]	2.7446	2.8439	3.0181	3.3771

**Table 7: Verification of  $\bar{\omega}$  (nx=0, L/h=20, R/h=infinity)**

$n_z$	Theory	1-0-1	2-1-2	1-1-1	1-2-1
0	Present	5.5749	5.5749	5.5749	5.5749
	Nguyen et al. [32]	5.4603	5.4603	5.4603	5.4603
	Vo et al. [33]	5.4603	5.4603	5.4603	5.4603
0.5	Present	4.3830	4.5042	4.6126	4.7849
	Nguyen et al. [32]	4.3132	4.4278	4.5315	4.6972
	Vo et al. [33]	4.3148	4.4290	4.5324	4.6979
1	Present	3.7636	3.9354	4.0983	4.3638
	Nguyen et al. [32]	3.7147	3.8768	4.0328	4.2889
	Vo et al. [33]	3.7147	3.8768	4.0328	4.2889
2	Present	3.2088	3.3913	3.5919	3.9411
	Nguyen et al. [32]	3.1764	3.3465	3.5389	3.8769
	Vo et al. [33]	3.1764	3.3465	3.5389	3.8769
5	Present	2.8608	2.9640	3.1537	3.5472
	Nguyen et al. [32]	2.8440	2.9311	3.1111	3.4921
	Vo et al. [33]	2.8439	2.9310	3.1111	3.4921

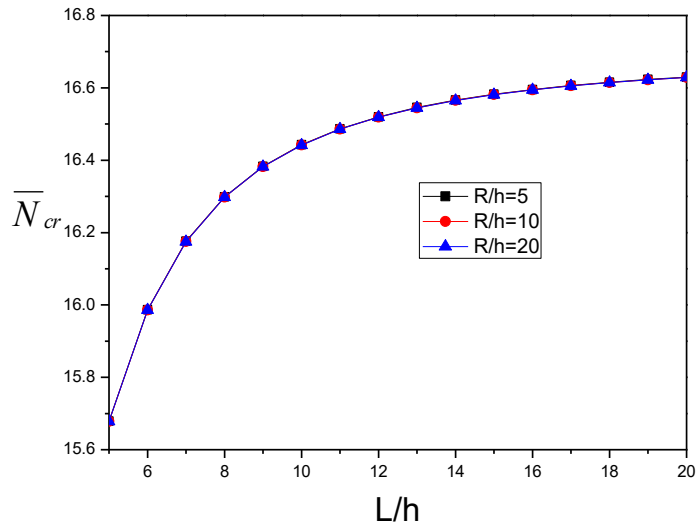


Figure 04: Effect of (L/h) on  $\bar{N}_{cr}$  (2-1-2,  $n_z=n_x=1$ )

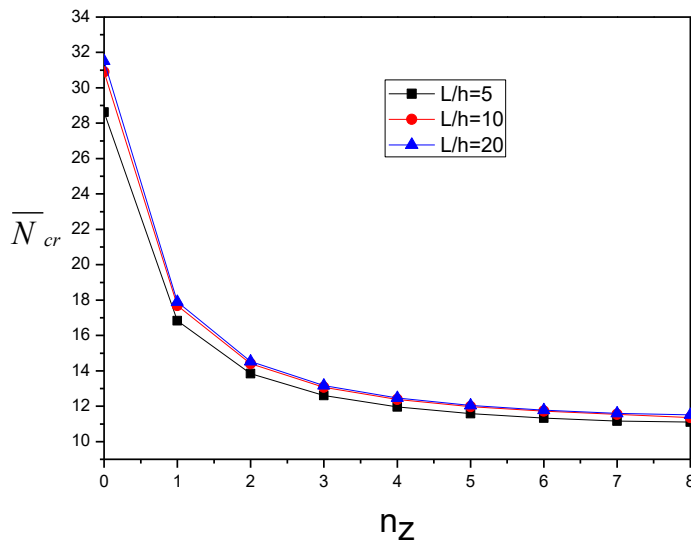


Figure 05: Effect of grading index  $n_z$  on  $\bar{N}_{cr}$  (1-1-1,  $n_x=1$ , R/h=5)

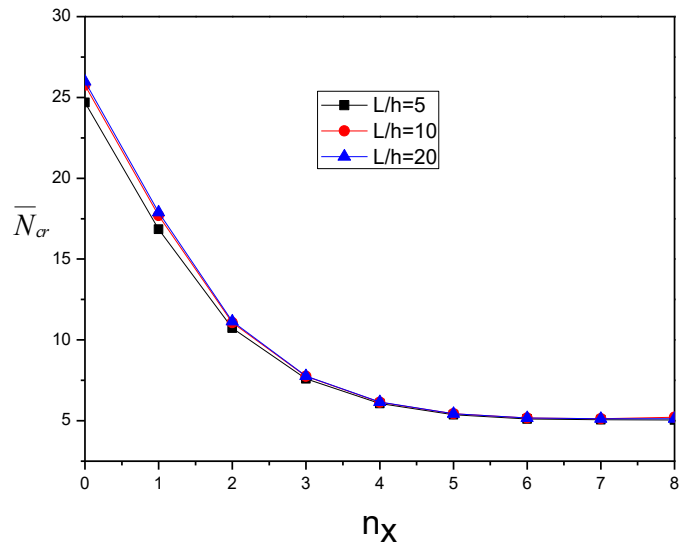


Figure 06: Effect of grading index  $n_x$  on  $\bar{N}_{cr}$  (1-1-1,  $n_z=1$ ,  $R/h=5$ )

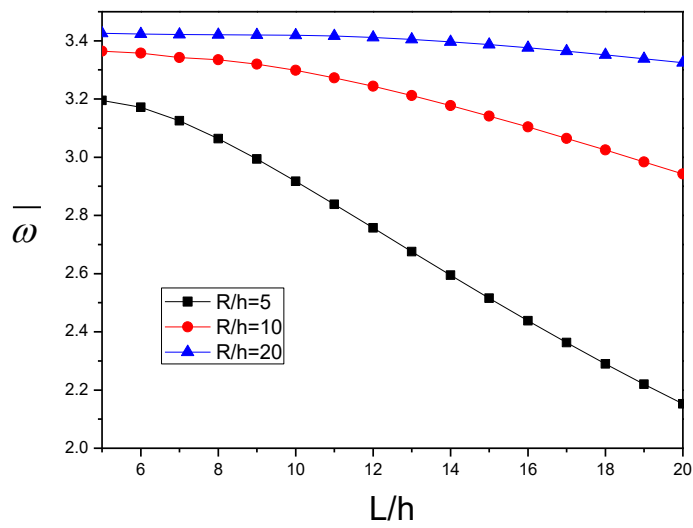


Figure 07: Effect of ( $L/h$ ) on  $\bar{\omega}$  (2-1-2,  $n_z=n_x=1$ )

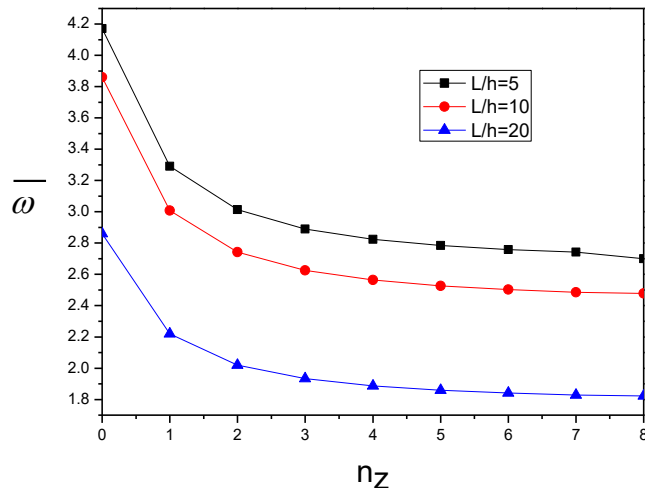


Figure 08: Effect of grading index  $n_z$  on  $\bar{\omega}$  (1-1-1,  $n_x=1$ ,  $R/h=5$ )

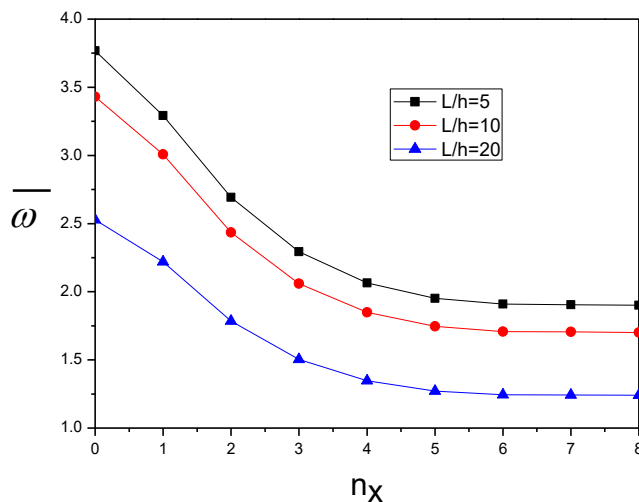


Figure 09: Effect of grading index  $n_x$  on  $\bar{\omega}$  (1-1-1,  $n_z=1$ ,  $R/h=5$ )

## 5. Conclusion

This study aims to analyze bending, buckling and free vibration response of BDFG curved sandwich beams. A quasi-3D high-shear deformation formulation involving three unknowns is employed to conduct this analysis by considering the stretching effect. According to the results of the present study, the following conclusion can be drawn as follows:

- Increasing the values of radius of curvature  $R/h$  ratio leads to a reduction in the axial displacement, regardless of the type of sandwich, the material composition of the beam (variation of  $n_x$  and  $n_z$ ) and the slenderness ratio ( $L/h$ ) used.
- The deflection values are not affected by the variation of the radius of curvature values. The axial stresses are only slightly affected by this variation, where a very slight increase can be noticed,

- For the same values of L/h and R/h ratios as well as the material composition of the beam, the lowest values of displacements and stresses are obtained for the sandwich type (1-2-1).
- The non-dimensional critical buckling load increases slightly with increasing (L/h) ratio.
- The increase in  $n_z$  and  $n_x$  indexes reduce substantially the nondimensional critical buckling load.
- The nondimensional fundamental natural frequency diminishes with increasing the indexes.

Further work can be performed using the present formulation, for example examination of curved beams/plates with variable section or using other kinds of materials and other models [34, 35].

### Declarations Conflict of interest

The authors declare that they have no known competing financial interests or personal relationships that could have appeared to influence the work reported in this paper.

### Acknowledgements:

The Authors extend their appreciation to the Deanship Scientific Research at King Khalid University for funding this work through large group Research Project under grant number: RGP2/422/44.

### References

- [1] Z.-Q. Wan, S.-R. Li, H.-W. Ma, Geometrically nonlinear analysis of functionally graded Timoshenko curved beams with variable curvatures, *Advances in Materials Science and Engineering*, Vol. 2019, No. 1, pp. 6204145, 2019.
- [2] Y. L. Pei, L. Li, A simplified theory of FG curved beams, *European Journal of Mechanics-A/Solids*, Vol. 85, pp. 104126, 2021.
- [3] A. Fereidoon, M. Andalib, H. Hemmatian, Bending analysis of curved sandwich beams with functionally graded core, *Mechanics of Advanced Materials and Structures*, Vol. 22, No. 7, pp. 564-577, 2015.
- [4] S. Stoykov, Buckling analysis of geometrically nonlinear curved beams, *Journal of Computational and Applied Mathematics*, Vol. 340, pp. 653-663, 2018.
- [5] N. Mohamed, M. Eltaher, S. Mohamed, L. Seddek, Numerical analysis of nonlinear free and forced vibrations of buckled curved beams resting on nonlinear elastic foundations, *International Journal of Non-Linear Mechanics*, Vol. 101, pp. 157-173, 2018.
- [6] W. Li, R. Geng, S. Chen, H. Huang, Geometrically exact beam element with predefined stress resultant fields for nonlinear analysis of FG curved beams with discontinuous stiffness, *Composite Structures*, Vol. 276, pp. 114437, 2021.
- [7] W. Li, H. Ma, W. Gao, Geometrically exact beam element with rational shear stress distribution for nonlinear analysis of FG curved beams, *Thin-Walled Structures*, Vol. 164, pp. 107823, 2021.
- [8] H. Kurtaran, Large displacement static and transient analysis of functionally graded deep curved beams with generalized differential quadrature method, *Composite Structures*, Vol. 131, pp. 821-831, 2015.
- [9] A. S. Sayyad, Y. M. Ghugal, A sinusoidal beam theory for functionally graded sandwich curved beams, *Composite Structures*, Vol. 226, pp. 111246, 2019.
- [10] L. Jun, R. Guangwei, P. Jin, L. Xiaobin, W. Weigu, Free vibration analysis of a laminated shallow curved beam based on trigonometric shear deformation theory, *Mechanics Based Design of Structures and Machines*, Vol. 42, No. 1, pp. 111-129, 2014.
- [11] A.-T. Luu, J. Lee, Non-linear buckling of elliptical curved beams, *International Journal of Non-Linear Mechanics*, Vol. 82, pp. 132-143, 2016.
- [12] T. Ye, G. Jin, Z. Su, A spectral-sampling surface method for the vibration of 2-D laminated curved beams with variable curvatures and general restraints, *International Journal of Mechanical Sciences*, Vol. 110, pp. 170-189, 2016.
- [13] C. Thurnherr, R. M. Groh, P. Ermanni, P. M. Weaver, Higher-order beam model for stress predictions in curved beams made from anisotropic materials, *International Journal of Solids and Structures*, Vol. 97, pp. 16-28, 2016.

- [14] P. V. Avhad, A. S. Sayyad, On the static deformation of FG sandwich beams curved in elevation using a new higher order beam theory, *Sādhanā*, Vol. 45, No. 1, pp. 188, 2020.
- [15] M.-O. Belarbi, A. Garg, M.-S.-A. Houari, H. Hirane, A. Tounsi, H. Chalak, A three-unknown refined shear beam element model for buckling analysis of functionally graded curved sandwich beams, *Engineering with Computers*, pp. 1-28, 2022.
- [16] M.-O. Belarbi, M. S. A. Houari, H. Hirane, A. A. Daikh, S. P. A. Bordas, On the finite element analysis of functionally graded sandwich curved beams via a new refined higher order shear deformation theory, *Composite Structures*, Vol. 279, pp. 114715, 2022.
- [17] U. Eroglu, Large deflection analysis of planar curved beams made of functionally graded materials using variational iterative method, *Composite Structures*, Vol. 136, pp. 204-216, 2016.
- [18] M. Lezgy-Nazargah, A finite element model for static analysis of curved thin-walled beams based on the concept of equivalent layered composite cross section, *Mechanics of Advanced Materials and Structures*, Vol. 29, No. 7, pp. 1020-1033, 2022.
- [19] M. Ganapathi, T. Merzouki, O. Polit, Vibration study of curved nanobeams based on nonlocal higher-order shear deformation theory using finite element approach, *Composite Structures*, Vol. 184, pp. 821-838, 2018.
- [20] T. Merzouki, M. Ganapathi, O. Polit, A nonlocal higher-order curved beam finite model including thickness stretching effect for bending analysis of curved nanobeams, *Mechanics of Advanced Materials and Structures*, Vol. 26, No. 7, pp. 614-630, 2019.
- [21] O. Polit, T. Merzouki, M. Ganapathi, Elastic stability of curved nanobeam based on higher-order shear deformation theory and nonlocal analysis by finite element approach, *Finite Elements in Analysis and Design*, Vol. 146, pp. 1-15, 2018.
- [22] M. Wang, Y. Liu, Elasticity solutions for orthotropic functionally graded curved beams, *European Journal of Mechanics-A/Solids*, Vol. 37, pp. 8-16, 2013.
- [23] B. Sahoo, K. Mehar, B. Sahoo, N. Sharma, S. K. Panda, Thermal post-buckling analysis of graded sandwich curved structures under variable thermal loadings, *Engineering with Computers*, pp. 1-17, 2023.
- [24] L. Li, X. Li, Y. Hu, Nonlinear bending of a two-dimensionally functionally graded beam, *Composite Structures*, Vol. 184, pp. 1049-1061, 2018/01/15/, 2018.
- [25] H. Liu, Q. Zhang, Nonlinear dynamics of two-directional functionally graded microbeam with geometrical imperfection using unified shear deformable beam theory, *Applied Mathematical Modelling*, Vol. 98, pp. 783-800, 2021.
- [26] H. Liu, S. Chen, Dynamic response of double-microbeam system made of transverse, longitudinal, and two-dimensional functionally graded materials, *The European Physical Journal Plus*, Vol. 136, No. 10, pp. 1-25, 2021.
- [27] A. Pydah, A. Sabale, Static analysis of bi-directional functionally graded curved beams, *Composite Structures*, Vol. 160, pp. 867-876, 2017.
- [28] A. Pydah, R. Batra, Shear deformation theory using logarithmic function for thick circular beams and analytical solution for bi-directional functionally graded circular beams, *Composite Structures*, Vol. 172, pp. 45-60, 2017.
- [29] J. Fariborz, R. Batra, Free vibration of bi-directional functionally graded material circular beams using shear deformation theory employing logarithmic function of radius, *Composite Structures*, Vol. 210, pp. 217-230, 2019.
- [30] P. R. Marur, 1999, *Fracture behaviour of functionally graded materials*, Auburn University,
- [31] K. Draiche, A. A. Bousahla, A. Tounsi, M. Hussain, An integral shear and normal deformation theory for bending analysis of functionally graded sandwich curved beams, *Archive of Applied Mechanics*, Vol. 91, pp. 4669-4691, 2021.
- [32] T.-K. Nguyen, T. T.-P. Nguyen, T. P. Vo, H.-T. Thai, Vibration and buckling analysis of functionally graded sandwich beams by a new higher-order shear deformation theory, *Composites Part B: Engineering*, Vol. 76, pp. 273-285, 2015.
- [33] T. P. Vo, H.-T. Thai, T.-K. Nguyen, A. Maheri, J. Lee, Finite element model for vibration and buckling of functionally graded sandwich beams based on a refined shear deformation theory, *Engineering structures*, Vol. 64, pp. 12-22, 2014.
- [34] E. Madenci, Free vibration analysis of carbon nanotube RC nanobeams with variational approaches, *Advances in nano research*, Vol. 11, No. 2, pp. 157-171, 2021.
- [35] E. Madenci, Free vibration and static analyses of metal-ceramic FG beams via high-order variational MFEM, *Steel and Composite Structures, An International Journal*, Vol. 39, No. 5, pp. 493-509, 2021.